Research Article

Experimental and Numerical Study on Ultimate Shear Load Carrying Capacity of Corroded RC Beams

Zhanzhan Tang [iD],[1] **Zhixiang He,**[1] **Zheng Chen,**[1] **Lingkun Chen** [iD],[1] **Hanyang Xue,**[1] **and Hanqing Zhuge**[2]

[1]*College of Civil Science and Engineering, Yangzhou University, Yangzhou 225127, China*
[2]*College of Civil Engineering and Architecture, Zhejiang University of Science & Technology, Hangzhou 310023, China*

Correspondence should be addressed to Lingkun Chen; lkchen@yzu.edu.cn

For an RC beam, the strength of steel rebar, the bonding strength between the concrete and reinforcement, and the bite action between the aggregates will deteriorate significantly due to corrosion. In the present study, 10 RC beams were designed to study the impact of corrosion on the shear bearing capacity. The mechanism of corrosion for stirrups and longitudinal bars and their effects were analyzed. Based on the existing experimental data, the correlation between the stirrup corrosion factor and the cross section loss rate was obtained. An effective prediction formula on the shear bearing capacity of the corroded RC beams was proposed and validated by the experimental results. Moreover, a numerical analysis approach based on the FE technique was proposed for the prediction of the shear strength. The results show that corrosion of the reinforcements could reduce the shear strength of the RC beams. The corrosion of stirrups can be numerically simulated by the reduction of the cross section. The formulae in the literature are conservative and the predictions are very dispersed, while the predictions by the proposed formula agree very well with the experiment results.

1. Introduction

Most of the infrastructures, e.g., buildings and bridges, are exposed to the natural environment for decades and unavoidably be corroded due to the corrosive environments around them. The corrosion of a reinforced concrete (RC) beam always leads to the strength loss of the reinforcement, the degradation of material mechanical properties, the descending of the bond strength between the reinforcements and concrete, and the decrease of biting force between the inclined crack of the aggregates, which are the main factors decreasing the durability of an RC structure. At present, most studies focused on the deterioration of bending strength of RC beams caused by corrosion, rather than the decrease of the shear strength. Therefore, it is very significant to study the influence of corrosion on the shear performance of the RC beams and to propose effective formulae to facilitate the shear bearing capacity evaluation process.

A series of studies have been carried out on the shear failure mechanism of the corroded RC beams. Corrosion is a continuous process, and the extension of cracks produced by structural corrosion is related to the loss of cross section [1–3]. Usually, the corrosion of reinforcement induces the crack initiation and propagation, and in turn, the development of cracks accelerates the corrosion [4]. Corrosion cracking also leads to the decrease of the bond strength between the reinforcement and concrete [5]. Khan et al. [6], Ye et al. [7], Zhao et al. [8], and Xu et al. [9] conducted experimental studies on the shear strength of corroded beams using the rapid electrochemical corrosion method. However, the effect of the longitudinal reinforcement corrosion was not involved. Sola et al. [3], Higgins et al. [10], Huo [11], and Wang et al. [12] investigated experimentally the shear performance of RC beams with consideration of the longitudinal reinforcement corrosion and the reduction of bond strength, while stirrup corrosion was ignored in

these studies. Dai et al. [13] and Xue et al. [14] discussed the effect of longitudinal reinforcement corrosion on the shear performance of RC beams through a targeted method. The abovementioned studies focused on the influences of either the longitudinal reinforcement corrosion or the stirrup corrosion. However, the combined effect of them on the shear bearing capacity was not analyzed.

Various improved prediction formulae and theoretical models were proposed after the establishment of the classical truss model, e.g., the variable angle truss model, the fixed pressure field theory, the truss-arch model, the pull-rod model, the limit equilibrium theory, the plasticity theory, and the statistical analysis. Based on the limit equilibrium theory, Xu et al. [9] analyzed the contribution proportions of the concrete and reinforcement to shear bearing capacity of the RC beams, in which the correlation coefficient of stirrup corrosion was introduced. El-Sayed [15] and Alaskar et al. [16] proposed a shear bearing capacity evaluation model for the corroded RC beams, in which the effective width of the member and the reduction of reinforcement cross section were considered. Zhao et al. [8] introduced the fitting empirical coefficient P_v to reduce the shear bearing capacity of noncorroded RC beams using the equivalent truss theory. Li et al. [17] considered the effective width of the geometrical dimension of the member after corrosion and the reduction of the yield strength of the longitudinal reinforcements when evaluating the shear bearing capacity of the corroded RC beams. Yu et al. [18] proposed a precise prediction formula which includes the angle of the critical inclined crack and the reduction of the cross section. However, most of the proposed formulae ignore either the impact of the longitudinal reinforcement corrosion or the deterioration of the stirrup and the decrease of the bonding strength. Therefore, the predictions are very conservative. Although the prediction of the formula proposed by Yu et al. [18] agrees well with the experiments, the method is very complicated when applying in engineering practice. Finite element analysis was carried out to study the mechanical performance of RC beams in recent years. Hawileh et al. [19] examined the critical parameters that influence the effectiveness of side-bonded EB-FRP systems through a newly developed finite element (FE) model. Naser et al. [20] discussed an advanced finite element simulation as a mean to understand and predict the performance of FRP-strengthened structures.

In this study, the influences of stirrups and longitudinal reinforcement corrosion on the shear bearing capacity of RC beams were experimentally and theoretically studied. A short-time test was adopted to facilitate the experiment, in which the longitudinal reinforcements were wrapped by a thin Teflon insulated film with perfect nonadhesion property to simulate the nonbonding effect, and the axial rust swelling crack was simulated by filling an acrylic plate. A more practical formula for the shear bearing capacity evaluation of corroded RC beams was proposed, whose effectiveness was validated by the experimental results. Moreover, numerical analysis based on the FE method was carried out and compared with the test results.

2. Structural Tests and Discussions

2.1. Shear Strength Test. A series of experimental studies on the shear bearing capacity of corroded RC beams have been carried out in the literature. However, the time costs of these experiments are extremely high; thus, in this study, a short-time test was adopted. The mechanical cutting method was adopted to simulate the stirrup corrosion, the wrapping of insulated Teflon film was adopted to simulate the unbonding effect of the corroded longitudinal reinforcements, and the filling of acrylic plate was adopted to simulate the rust expansion cracks. Sufficient bending reinforcements were utilized so that only shear failure could occur. The steel and concrete materials specified by the Japan JIS-G-3112-2004 standard [21] and the Japan Architectural Institute JASS5 standard [22] were used. In the test, 10 beams were designed. The specimens were divided into two groups, in which 2 specimens were designed for the stirrup corrosion and 2 specimens were designed with consideration of the bonding strength and 1 ordinary RC beam for comparison purpose in Group A. In Group B, 2 specimens were designed for simulating the combined effects of bond strength and rust swelling crack and 2 specimens were designed to simulate rust swelling crack and 1 ordinary beam for comparison. Table 1 lists the design parameters of the specimens, where η_1 and η_w are the cross section loss rates due to corrosion of the longitudinal reinforcements and stirrups, respectively. s and λ are the stirrup spacing and the shear span ratio, respectively.

The extent of the bond strength degradation can be determined by the corrosion level [23]. The unbonded longitudinal reinforcements can be converted to a mass loss rate. The relationship between the reduction factor of bond strength ξ and the mass corrosion rate of the reinforcement η_m is [24]

$$\xi = \begin{cases} 1.0 + 0.125 \times \eta_m, & \eta_m \leq 2.0\%, \\ 1.59 \times \eta_m^{-0.35}, & \eta_m > 2.0\%. \end{cases} \quad (1)$$

Similarly, the simulated rust swelling crack can be transformed into the corresponding area loss rate η_s ($\eta_s = \Delta A_{sm}/A_s$, where ΔA_{sm} and A_s are the average area loss and the original area of reinforcement, respectively). The relationship between ΔA_{sm} and the corrosive crack width w is [25]

$$w = 0.1916\Delta A_{sm} + 0.164. \quad (2)$$

Before the structural test, material tests were conducted. Figure 1(a) shows the tensile test of the reinforcements, in which a 50 kN universal testing machine was used. Four types of reinforcements with different diameters, including D6 (SD295), D10 (SD295), D13 (SD345), and D22 (SD490), were tested. The specimen ID of D6 indicates the nominal diameter of the steel bar, and SD295 in the parenthesis represents the strength grade of steel bar, which indicates the yield point or 0.2% guaranteed strength is greater than 295 MPa. Standard tensile tests were carried out on the steel bars in the same batch. Different mass loss rates of 0%, 20%, and 40% were considered by the cutting

TABLE 1: Specimen design parameters.

Group	No.	Dimension (mm)	s (mm)	λ	Corrosion	η_1 (%)	η_w (%)
A	A1	$125 \times 200 \times 1500$	125	2.94	No corrosion	0	0
	A2	$125 \times 200 \times 1500$	125	2.94	Stirrup corrosion	0	25.2
	A3	$125 \times 200 \times 1500$	125	2.94	Stirrup corrosion	0	44.2
	A4	$125 \times 200 \times 1500$	125	2.94	Longitudinal bar corrosion	23.1	0
	A5	$125 \times 200 \times 1500$	125	2.94	Longitudinal bar corrosion	41.1	0
B	B1	$150 \times 235 \times 2200$	180	2.93	No corrosion	0	0
	B2	$150 \times 235 \times 2200$	180	2.93	Longitudinal bar corrosion	20.0	0
	B3	$150 \times 235 \times 2200$	180	2.93	Longitudinal bar corrosion	26.0	0
	B4	$150 \times 235 \times 2200$	180	2.93	Longitudinal bar corrosion	44.1	0
	B5	$150 \times 235 \times 2200$	180	2.93	Longitudinal bar corrosion	69.4	0
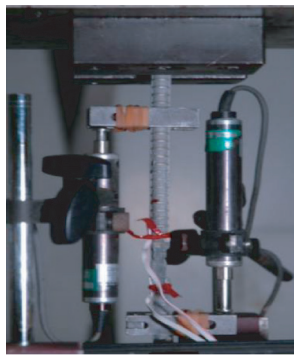
(a)
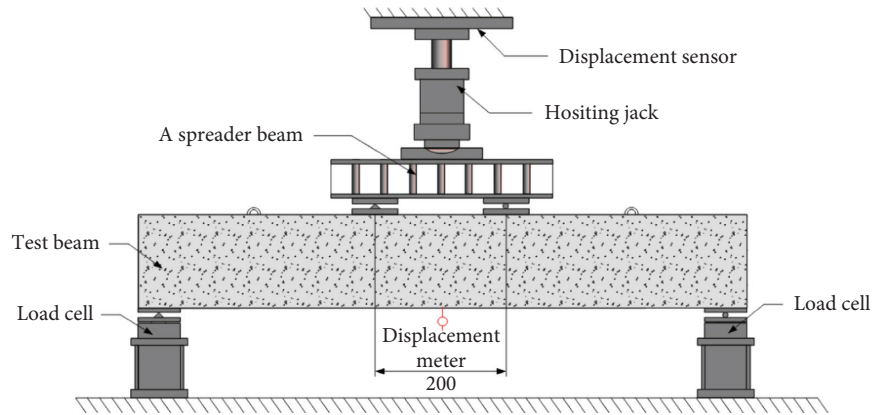
(b)

FIGURE 1: Material and structural tests. (a) Tensile tests of reinforcements. (b) Shear bearing capacity tests of beams.

TABLE 2: Mechanical properties of reinforcements.

Type	Grade	Effective yielding strength (MPa)	Effective ultimate strength (MPa)	Effective elastic modulus (GPa)
D6-0% mass loss rates	SD295	356	499	193
D6-20% mass loss rates	SD295	305	418	155
D6-40% mass loss rates	SD295	220	297	97
D10-0% mass loss rates	SD295	374	519	200
D13-0% mass loss rates	SD345	391	565	199
D22-0% mass loss rates	SD490	533	712	192

treatment for D6 steel bars. Table 2 shows the mechanical properties of the tested reinforcements. As it can be seen, the effective elastic modulus, the effective yielding strength, and ultimate strength decrease due to the cross section loss. Moreover, ordinary Portland cement was used to get a target compressive strength of 21 MPa for the concrete. Standard material tests were conducted using the cylinder blocks (ϕ100 mm $\times$ 200 mm), and the measured compressive and tensile strengths are 24.1 MPa and 2.28 MPa, respectively. Figure 1(b) shows the shear strength test of the corroded RC beams, in which a 2 MN mechanical universal testing machine and a TDS-7130 (version 1.3) recorder were used. The midspan vertical displacement, the longitudinal strain at the midspan of the beam bottom, and the stirrup strain in the shear-compression zone were measured during the test.

2.2. Effect of Corrosion on Shear Bearing Capacity. A typical shear failure mode was observed from the tests. The shear bearing capacity declines due to the corrosion of the stirrup and the longitudinal reinforcements. Figure 2 shows the relationship between the shear bearing capacity V_u of each beam and the corrosion ratio of the steel bars, in which the effects of the corrosion ratios of the stirrup η_w and the longitudinal reinforcement η_1 were revealed. It can be seen from the tests of Group A that the shear bearing capacities of A2 and A3 beams with corroded stirrups decrease remarkably. At the early stage of the corrosion, the shear capacity decreases slightly. As the corrosion level becomes severe, the shear strength decreases significantly. The shear bearing capacity of A3 beam with a stirrup mass loss rate of 44.2% is 62.35 kN, which is 21.4% lower than that of the noncorroded beam. Likewise, the shear strength of A5 beam

with a longitudinal reinforcement corrosion rate of 41.1% is only 58.25 kN, which is 26.6% lower than its original strength. The tests of Group B show that except for beam B4, the shear bearing capacity decreases with the increase of the corrosion level.

3. Shear Bearing Capacity Evaluation of Corroded RC Beams

3.1. Models in the Codes. In the Chinese and American specifications, the shear resistances of the longitudinal reinforcements and the concrete are separately considered for the RC beams, indicating the classical truss model is adopted. The shear strength prediction formula of RC beams under a concentrated load stipulated by the Chinese specifications is [26]

$$V_{cs} = \frac{1.75}{\lambda + 1.0} f_t b_w h_0 + \frac{h_0}{s} A_{sw} f_{yw}, \quad (3)$$

where V_{cs} is the shear strength of the beam, f_t is the concrete tensile strength, b_w and h_0 are the width and effective height of the cross section, respectively, A_{sw} is the cross section area of the stirrup, and f_{vw} is the yield strength of the stirrup.

The shear strength prediction formula of an RC beam with stirrups in the American standard is [27]

$$V_{cs} = \varphi(V_c + V_s) = \varphi\left(0.17\omega\sqrt{f_c'}\,b_w h_0 + \frac{A_{sw} f_{yw} h_0}{s}\right), \quad (4)$$

where φ is the strength reduction coefficient of 0.85, V_c and V_s are shear strength provided by concrete and stirrups, respectively, ω is the concrete correction coefficient of 1.0, and f_c is the compressive strength of the standard concrete cylinder.

The variable angle truss model is adopted by the European standard, in which the concrete is treated as a diagonal compressive bar. The angle between the equivalent diagonal bar and the longitudinal axis of the beam is variable within a prescribed range [28]. Figure 3 shows the variable angle truss model, where θ is the inclination angle between the effective compressive rod of the concrete and the longitudinal axis and α is the angle between the effective tension rod caused by the stirrups and the longitudinal axis. F_{cs} is the compression force of the equivalent compression rod caused by concrete, and F_{sw} is the tensile force of the equivalent tension rod caused by the stirrup. $z(=0.9h_0)$ is the inner lever arm corresponding to the maximum bending moment in the element under consideration.

According to the specifications, cot θ ranges from 1.0 to 2.5, and the shear strength of the RC beam can be predicted by

$$V_{Rd} = V_{Rd,c} + V_{Rd,s} = \frac{1}{\beta}\left[C_{Rd,c}k\left(100\rho_l f_{ck}\right)^{(1/3)} b_w h_0\right] + \frac{1}{\beta}\left[\frac{0.9h_0 f_{yw} A_{sw}}{s}\left(\cot\theta + \cot\alpha\right)\sin\alpha\right],$$

$$\beta = \begin{cases} 0.25, & a_v < 0.5h_0, \\[2mm] \dfrac{a_v}{2h_0}, & 0.5h_0 \le a_v \le 2h_0, \\[2mm] 1, & a_v > 2h_0, \end{cases} \quad (5)$$

where V_{Rd} is the shear strength of RC beams, $V_{Rd,c}$ and $V_{Rd,s}$ are shear strength provided by concrete and stirrups, respectively. $C_{Rd,c} = 0.18/\gamma_c$, in which γ_c (=1.5) is the material coefficient of concrete. $k = 1 + \sqrt{200}/h_0 \le 2$, and ρ_1 is the longitudinal reinforcement ratio. f_{ck} is the characteristic compressive strength of concrete, $f_{ck} = f_{cu,k}/1.226$ [29]. $f_{cu,k}$ is the standard value of the cubic concrete compressive strength. β is the coefficient of the shear span ratio, and a_v is the horizontal distance between the concentrated load point and the bearing support.

The partial factor of the shear resistance contributed by the stirrups is taken as 1.0 in the Chinese and American specifications, indicating the angle between the diagonal compressive bar and the longitudinal axis is a constant value of 45°. Table 3 shows the shear strength errors between the experimental results and the predictions by the formulae in the standards [29], where K_p is the ratio of the experimental strength to the prediction by the formulae and μ_{kp} and σ_{kp} are, respectively, the average value and discrete coefficient of

K_p. It is found that the prediction of the European standard is more accurate due to the consideration of the angle θ, while the predictions based on the Chinese and American standards are very conservative.

4. Proposed Formula for Prediction of Shear Bearing Capacity

As the variable angle truss theory is more effective, the contributions of the concrete and stirrups to the shear resistance are discussed in this section. In the theory, the concrete between the diagonal cracks is treated as a pressure rod to resist the compressive force, while the stirrups are equivalent to an upper chord, and the bottom longitudinal bars are considered as a lower chord to resist the tensile force. In order to ensure that the stirrups can reach their yield strength before the concrete crushing, the EC2 stipulates that $21.8° < \theta < 45°$ ($1.0 \le \cot\theta \le 2.5$) [28]. Supposing that $\alpha = 90°$, then
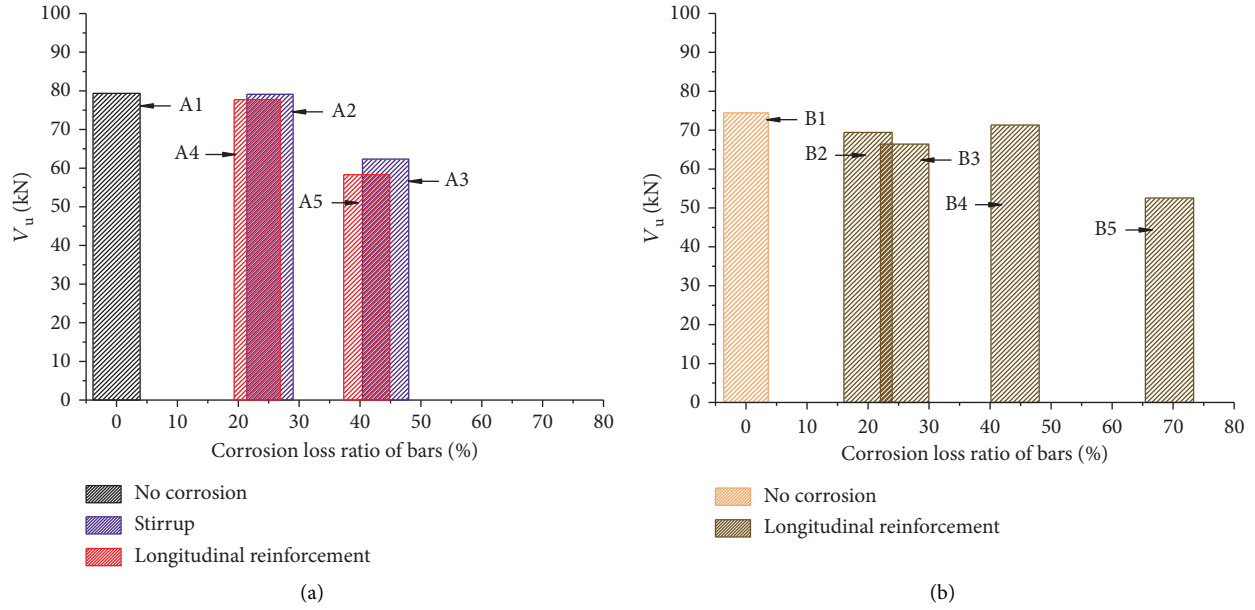
(a)

(b)

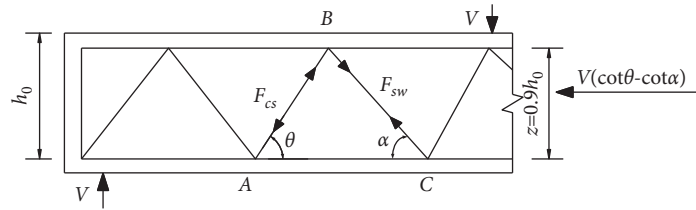FIGURE 2: Shear strength versus the corrosion ratio. Test results of (a) Group A and (b) Group B.

FIGURE 3: Variable angle truss model in Eurocode 2.

TABLE 3: Statistical parameters of K_p.

Parameters	Chinese standard	American standard	European standard
μ_{kp}	1.4403	1.8403	0.9697
σ_{kp}	0.2319	0.3008	0.2297

$$\cot \theta = \sqrt{\frac{\alpha_{cv} v_1 f_{cd}}{\rho_w f_{yw}} - 1},$$

$$v_1 = \begin{cases} 0.6, & f_{ck} \leq 60 \text{MPa}, \\ 0.9 - \dfrac{f_{ck}}{200} > 0.5, & f_{ck} > 60 \text{MPa}, \end{cases} \tag{6}$$

where α_{cv} is a coefficient considering the stress state of the compression rod, and $\alpha_{cv} = 1$ for nonprestressed structures. ρ_w is the stirrup ratio, v_1 is the reduction factor with consideration of the concrete cracking strength, and f_{cd} ($=\alpha_{cc} f_{ck}/\gamma_c$) is the design value of the concrete compression force in the direction of the longitudinal member axis. α_{cc} is

the influencing factor of the long-term action effect of concrete, which can be taken as 0.85 [28].

As surface spalling of the concrete may occur due to severe corrosion of the reinforcements, the width of the beam should be reduced. According to the suggestions of Higgins et al. [10], the effective width b_{wc} can be calculated by

$$b_{wc} = \begin{cases} b_w, & \eta_w \leq 30\%, \\ b_w - 2(c + d_{sw}) + \dfrac{s}{5.5}, & \eta_w > 30\%, \ s \leq 5.5c, \\ b_w - \dfrac{5.5}{s}(c + d_{sw})^2, & \eta_w > 30\%, \ s > 5.5c, \end{cases} \tag{7}$$

where c is the thickness of the concrete cover and d_{sw} is the diameter of the stirrups. The relationship between the mass loss rate η_m and the area loss rate η_s is

$$\eta_s = \begin{cases} 0.015 + 0.97\eta_m, & \eta_m \leq 10\%, \\ 0.062 + 0.95\eta_m, & \eta_m > 10\%. \end{cases} \quad (8)$$

A theoretical prediction formula for shear strength evaluation of the corroded RC beams is proposed, in which the factors of ϕ and γ to, respectively, consider the corrosion impacts of the longitudinal reinforcements and the stirrups are involved:

$$\begin{aligned} V_{Rc} &= \phi V_{Rd,c} + \gamma V_{Rd,s} \\ &= \frac{1}{\beta}\left[\phi C_{Rd,c}k\left(100\rho_l f_{ck}\right)^{(1/3)}b_{wc}h_0 + \gamma\frac{0.9h_0 f_{ywc}A_{sw}}{s}\cot\theta\right], \end{aligned} \quad (9)$$

where V_{Rc} is the shear strength of corroded RC beams, b_{wc} and f_{ywc} ($= f_{yw}(1 - 1.077\eta_s)/(1 - \eta_s)$) are, respectively, the effective width of the section and the nominal yield strength of the steel bars after corrosion. $\cot\theta$ can be calculated using equation (6), in which ρ_w and f_{yw} can be replaced by ρ_{wc} and f_{ywc} in consideration of corrosion. The corrosion factors of ϕ can be obtained by [11]

$$\phi = \begin{cases} 1.0, & \eta_l \leq 5\%, \\ 1.098 - 1.96\eta_l, & \eta_l > 5\%. \end{cases} \quad (10)$$

As the conditions of the stirrups have a significant effect on the shear performance of the corroded RC beams, the correlation between parameters γ and η_w is discussed. Thus, 10 tests in this study and 118 tests in the literature are selected for further analysis [9–12, 30–34]. Table 4 lists the summary of the experimental results on shear strength of the RC beams with corroded stirrups, in which f_c is the design value of the concrete axial compressive strength and N is the number of tests in each literature.

Figure 4 shows the collection of the experimental data and the fitting relation between the parameters γ and η_w. The experimental results show that the shear strength is almost unaffected when the corrosion rate is relatively small. Therefore, γ is taken as 1.0 in this study when η_w is less than 10%, indicating the shear strength of the corroded RC beam can retain the original strength as the noncorroded one. When the corrosion rate becomes larger, the shear strength decreases gradually, and a linear fitting relation between parameters γ and η_w is adopted:

$$\gamma = \begin{cases} 1.0, & \eta_w \leq 10\%, \\ 1.076 - 0.76\eta_w, & \eta_w > 10\%. \end{cases} \quad (11)$$

4.1. Verification of Prediction Formula. The ratio K_p ($= V_{u,\exp}/V_u$) between the experimental strength $V_{u,\exp}$ and the predicted value V_u is obtained. Meanwhile, the mean value and the dispersion coefficient of the ratio are calculated. Figure 5 shows the comparison between the experimental and the predicted shear strengths using different

theoretical models, where μ_{kp} is the mean value of the ratio K_p and σ_{kp} is the corresponding coefficient of variation. The predicted strengths obtained from the theoretical models are different from each other. The formula proposed by Yu is based on the modified pressure field theory, in which the influence of corrosion on the angle of critical inclined crack, geometric reduction, and the stirrup ratio is considered. Therefore, the predictions are in a good agreement with the test values. The mean value of K_P is 1.0785 with a dispersion coefficient of 0.2834. However, complicated iterative computation is required in Yu's model, making it very difficult for engineering practice. Huo's model is based on the truss-arch theory, and the accuracy of the prediction is lower than Yu's model. The model proposed by El-Sayed is based on the American standard, which considers the reduction of the cross section and the effective shear section caused by corrosion. Nevertheless, the inclination of the crack in this model is assumed as a fixed value of 45°, so the predictions are rather conservative. The strength is a sum of the shear resistances of the stirrup and the concrete in the Xu and Li's models. The angle between the baroclinic bar and the longitudinal axis is also a constant value, and the corrosion of the longitudinal reinforcement is not considered. Thus, conservative predictions are obtained. Noticeably, the average value of K_p is 1.0027 with a dispersion coefficient of 0.172 in the proposed model, indicating the highest precision with a relatively small dispersion can be achieved by the proposed formula in this study.

4.2. Numerical Simulation of Shear Capacity of Corroded Beams. Finite element analysis is carried out to study the shear failure of the corroded RC beam in this section. Figure 6 shows the three-dimensional FE model of the RC beam. Commercial software ABAQUS was adopted for the numerical analysis. The concrete beam was modeled by 3D solid element (C3D8). The longitudinal reinforcements and stirrups were modeled by truss elements (T3D2). The plastic-damage constitutive model was adopted for the simulation of the concrete material, and the bilinear plastic constitutive model was used for the mechanical behavior of the reinforcements [35–37]. The cross section reduction method was adopted for the simulation of the reinforcement corrosion [38–41]. The coupling interaction between the longitudinal reinforcement and the concrete was utilized to control they were fully bonded or disconnected [42]. The meshing of the structure was carried out using the structured meshing method during the FE modelling.

Figure 7 shows the comparison of the load-deflection curves obtained from the numerical and the test results. It can be seen that the numerical results of both the test beams in Group A and Group B (FEM) are in good agreement with the experimental results (EXP). The effect of the corrosion can be well simulated by the section reduction of the rebar and the coupling interaction between the reinforcement and concrete beam.

128 models of the corroded RC beams in the literature with stirrups were created, and the shear bearing capacity was computed. Figure 8 shows the comparison between the

TABLE 4: Summary of experimental data on shear capacity of corroded beams with stirrups.

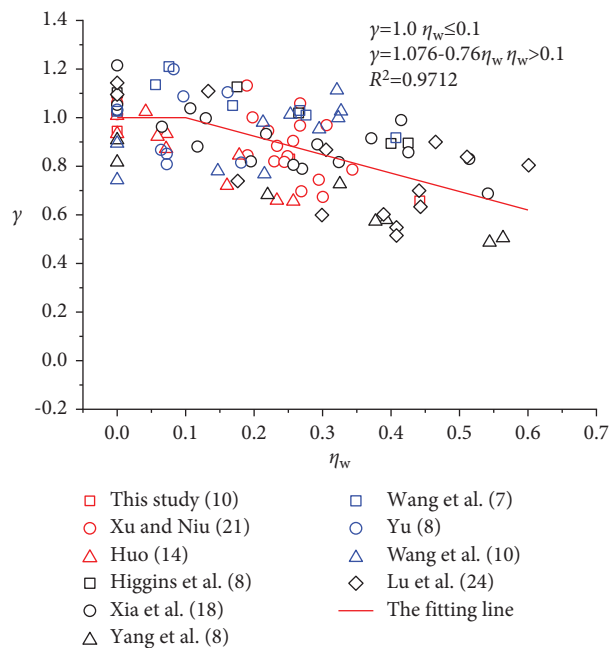| Data source	N	Beam no.	f_c (MPa)	b_w (mm)	h_0 (mm)	ρ_l (%)	ρ_w (%)	f_{yw} (MPa)	A_{sw} (mm^2)	s (mm)	λ
This study	10	A1~A5	14.3	125	170	3.6	0.41	360	63.4	125	2.94
		B1~B5	14.3	150	205	2.5	0.23	360	63.4	180	2.93
Xu et al. [9]	21	A/B/A2~C2	15.06~16.25	120	200	1.92	0.32	275	57	150	2.00
		A3~C3/A5~C5	15.06~16.25	120	200	1.92	0.32	275	57	150	2.00
		C/A1~A3	15.06~16.25	120	200	1.92	0.32	275	57	150	1.00
		A4~C4/A6~C6	15.06~16.25	120	200	1.92	0.32	275	57	150	1.00
Higgins et al. [10]	8	8RA/8RD	17.58	254	521	1.9	0.196	585	101	203	2.04
		10RA~10RD	20.04	254	521	1.9	0.157	585	101	254	2.04
		12RA/12RD	17.76	254	521	1.9	0.13	585	101	305	2.04
Huo [11]	14	L1~L14	9.6	100	170	1.94	0.44	324	66	150	1.50
Wang et al. [12]	10	BC2.0-1~5	18.29~26.74	150	150	1.29	0.31	441.5	57	150	2.00
		BC3.0-1~5	18.29~26.74	150	150	1.29	0.31	441.5	57	200	3.00
Xia et al. [30]	18	A-0~A-5	12.97	120	200	2.68	0.253	321.8	67.2	100	1.50
		B-0~B-5	12.97	120	200	2.68	0.19	321.8	67.2	100	1.50
		C-0~C-5	12.97	120	200	2.62	0.475	463.9	92	150	1.50
Yang et al. [31]	8	1.5-1~1.5-4	21.27	150	260	2.62	0.475	482	101	150	1.50
		L1-1~L1-4	21.27	150	260	2.62	0.561	482	101	150	1.00
Wang et al. [32]	7	0#~6#	16.91~18.32	250	455	2.34	0.447	337.9	66	200	1.74
Yu [33]	8	JL-L0~JL-L5	11.02~12.83	180	260	2.34	0.447	280	57	120	2.22
		HJL-L1/L3/L5	11.02~12.83	180	260	1.63	0.12	280	57	120	2.22
Lu et al. [34]	24	X1/X2	19.49	200	275	2.15	0.19/0.14	339	57	150/200	2/2.5
		X3/X4	19.49	200	275	2.15	0.2/0.25	373	101	250/200	3/3.5
		X5/X6	19.49	200	275	2.15	0.19/0.14	458	57	150/200	2/2.5
		X7/X8	19.49	200	275	2.15	0.2/0.25	433	101	250/200	3/3.5
		X9/X10	19.49	200	275	2.15	0.19/0.14	476	57	150/200	2/2.5
		X11/X12	19.49	200	275	2.15	0.2/0.25	524	101	250/200	3/3.5
		Y1/Y2	23.86	200	275	2.15	0.19/0.14	339	57	150/200	2/2.5
		Y3/Y4	23.86	200	275	2.15	0.2/0.25	373	101	250/200	3/3.5
		Y5/Y6	23.86	200	275	2.15	0.19/0.14	458	57	150/200	2/2.5
		Y7/Y8	23.86	200	275	2.15	0.2/0.25	433	101	250/200	3/3.5
		Y9/Y10	23.86	200	275	2.15	0.19/0.14	476	57	150/200	2/2.5
		Y11/Y12	23.86	200	275	2.15	0.2/0.25	524	101	250/200	3/3.5

$\gamma=1.0 \ \eta_w \leq 0.1$
$\gamma=1.076-0.76\eta_w \ \eta_w>0.1$
$R^2=0.9712$

□ This study (10)   □ Wang et al. (7)
○ Xu and Niu (21)   ○ Yu (8)
△ Huo (14)   △ Wang et al. (10)
□ Higgins et al. (8)   ◇ Lu et al. (24)
○ Xia et al. (18)   — The fitting line
△ Yang et al. (8)

FIGURE 4: Correlation between γ and η_w.
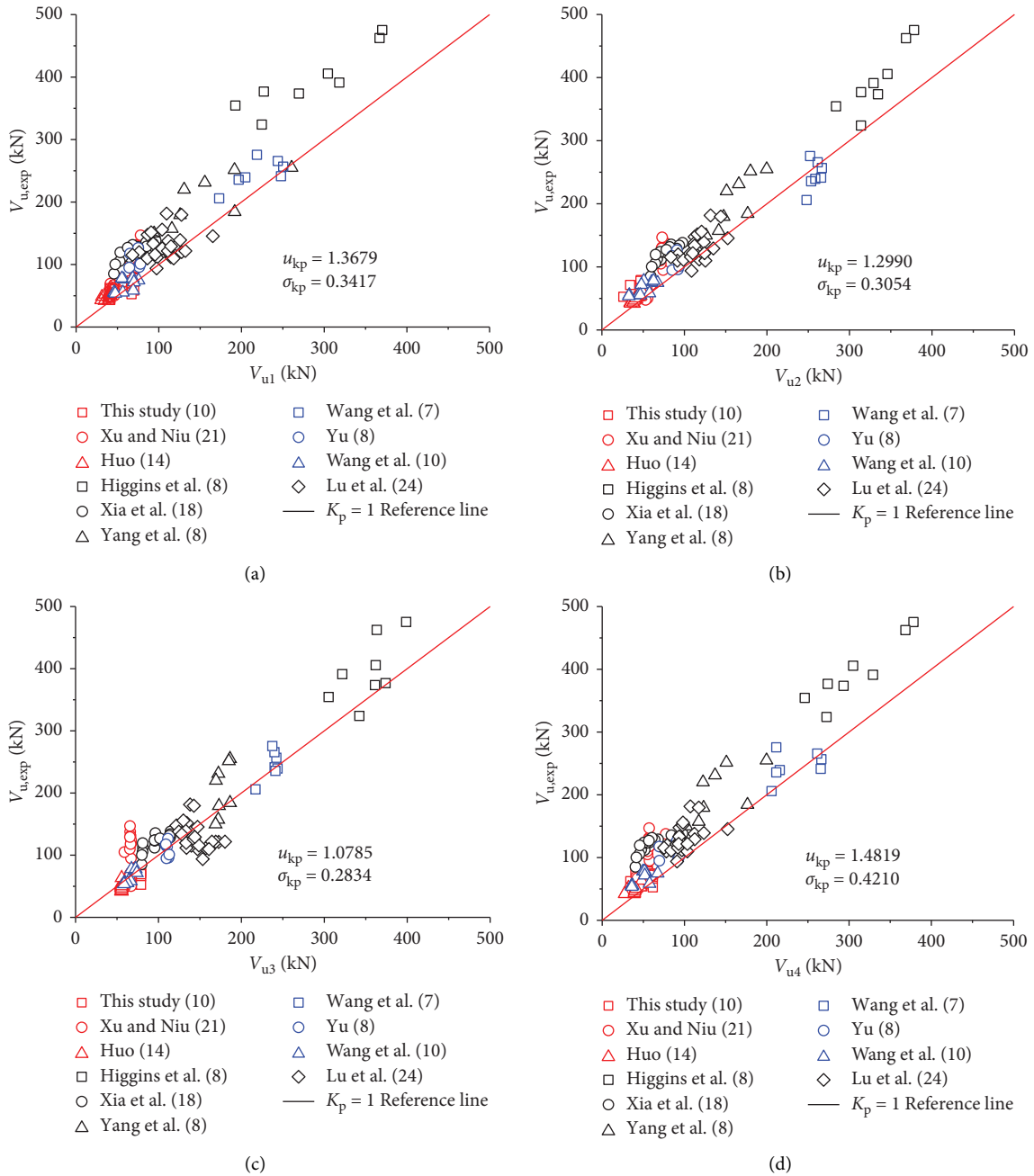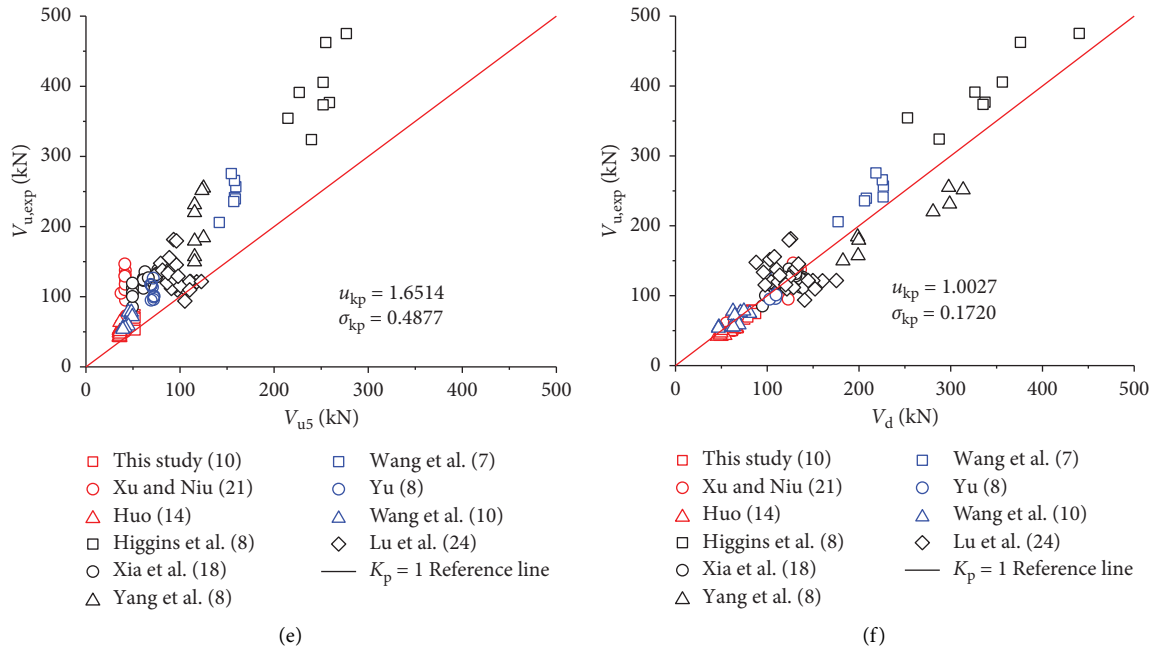
(a)

(b)

(c)

(d)

FIGURE 5: Continued.

(e)

(f)

FIGURE 5: Comparison between the experimental and theoretical shear strength of the corroded RC beams. (a) V_{u1} predicted by Xu's model. (b) V_{u2} predicted by Huo's model. (c) V_{u3} predicted by Yu's model. (d) V_{u4} predicted by Li's model. (e) V_{u5} predicted by El-Sayed's model. (f) V_d predicted by the proposed model in this study.
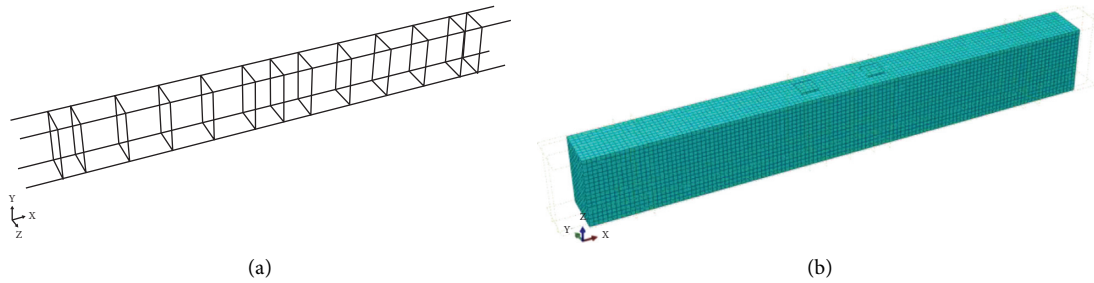

(a)

(b)

FIGURE 6: FE model of the corroded RC beam. (a) Framework of the reinforcement. (b) Mesh of the model.
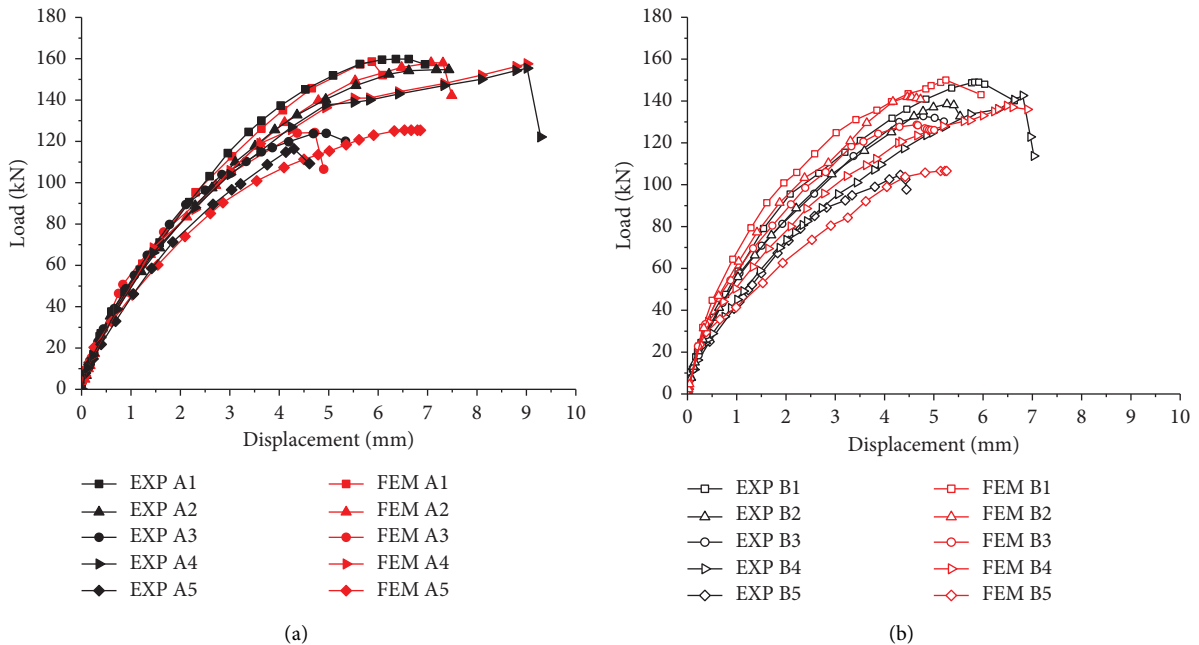

(a)

(b)

FIGURE 7: Comparison between the numerical and experimental results. Load-deflection curves of beams in (a) Group A and (b) Group B.
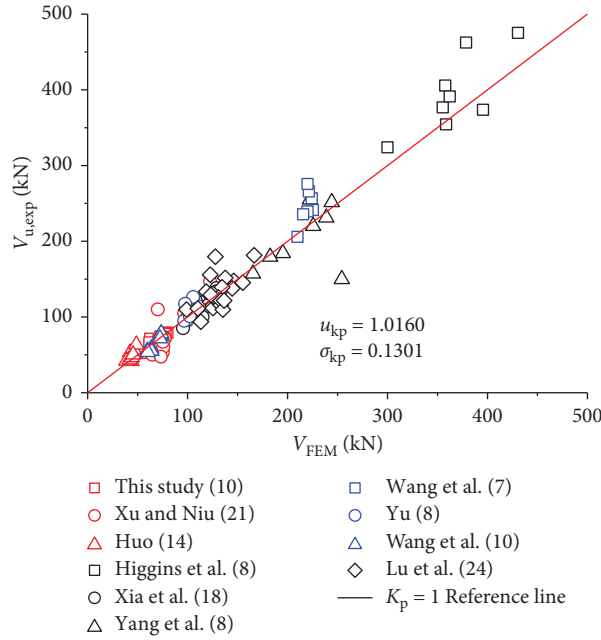
FIGURE 8: Comparison between numerical and experimental results for 128 specimens.
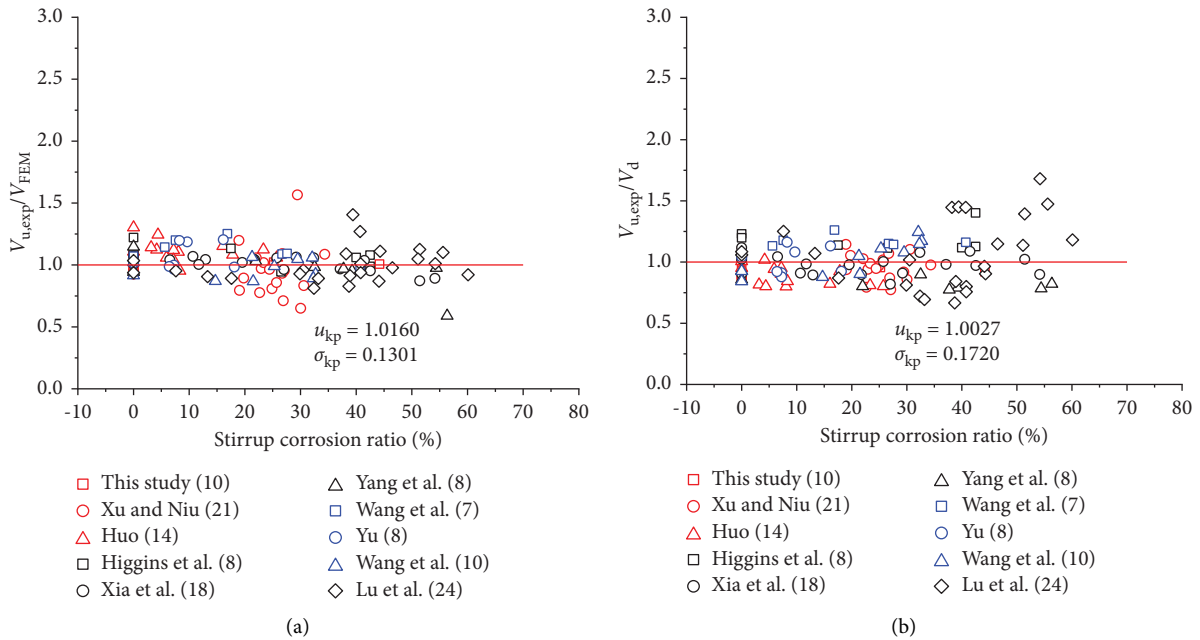

(a)

(b)

FIGURE 9: Comparison of the numerical results and the experimental or theoretical results. Ratios of (a) $V_{u,\exp}/V_{FEM}$ and (b) $V_{u,\exp}/V_d$.

numerical and the experiment results of the shear strength. Electrochemical corrosion or other fast corrosion methods were adopted by most of tests in the literature. Therefore, the corroded reinforcement was computed using the cross section reduction technique during the numerical analysis. As it can be seen, the mean value of the ratio K_p ($= V_{FEM}/V_{u,\exp}$) is 1.0160 and the corresponding dispersion coefficient is 0.1301.

K_p is higher than the mean value predicted by the proposed formula, but the dispersion coefficient is lower, indicating that the numerical results using the FE method are more accurate than the proposed theoretical method.

Figure 9 shows the comparison of the numerical results and the experimental or theoretical results. It can be found that it is feasible to evaluate the shear strength of the

corroded beam by the cross section reduction method and the interaction technique. Moreover, the effectiveness of the proposed formula is verified by the numerical analysis.

5. Conclusions

The shear bearing capacity of the corroded RC beams was experimentally and numerically studied. A short-time test was adopted to facilitate the experimental study, and a more practical formula for the shear strength evaluation was proposed and validated by the experimental data. Moreover, numerical analysis based on the FE method was carried out and compared with the test results. The following conclusions can be drawn:

(1) Stirrup corrosion has a significant effect on the shear strength of the RC beams, and the shear strength decreases gradually along with the increase of the corrosion rate. The axial rust swelling crack and the degradation of the bond strength due to longitudinal reinforcement corrosion can also decrease the shear strength. Moreover, the wrapping of the thin Teflon insulated film on the longitudinal reinforcements is an effective way to simulate the nonbonding effect, and the filling of an acrylic plate is feasible for the simulation of rust swelling crack in the short-time test.

(2) Most of the existing theoretical models for the shear strength estimation of the corroded RC beams are conservative and the predicted results are very dispersed, while the models with relatively higher accuracy are complicated in application. As the corrosion effects of the longitudinal reinforcement and the stirrup are both considered, the predictions by the proposed formula in this study are in good agreement with the experimental results, and the formula is very simple and easy for engineering application.

(3) The numerical results based on the FE technique agree very well with the experimental results, which indicates that the corrosion effect can be well simulated by the cross section reduction of the reinforcements and the coupling interaction between the reinforcement and the concrete beam. Moreover, the proposed prediction formula is validated by the numerical simulations.

Data Availability

The data are included within the article.

Conflicts of Interest

The authors declare that there are no conflicts of interest regarding the publication of this paper.

Acknowledgments

References

[1] T. Vidal, A. Castel, and R. François, "Analyzing crack width to predict corrosion in reinforced concrete," *Cement and Concrete Research*, vol. 34, no. 1, pp. 165–174, 2004.

[2] Y. X. Zhao, J. Chen, and W. L. Jin, "Design of shear strengths of corroded reinforced concrete beams," *International Journal of Modelling, Identification and Control*, vol. 7, no. 2, pp. 190–198, 2009.

[3] E. Sola, J. Ožbolt, G. Balabanić, and Z. M. Mir, "Experimental and numerical study of accelerated corrosion of steel reinforcement in concrete: transport of corrosion products," *Cement and Concrete Research*, vol. 120, pp. 119–131, 2019.

[4] L. Huang, H. Ye, X. Jin, N. Jin, and Z. Xu, "Corrosion-induced shear performance degradation of reinforced concrete beams," *Construction and Building Materials*, vol. 248, Article ID 118668, 2020.

[5] Y. Moodi, M. R. Sohrabi, and S. R. Mousavi, "Corrosion effect of the main rebar and stirrups on the bond strength of RC beams," *Structure*, vol. 32, pp. 1444–1454, 2021.

[6] I. Khan, R. François, and A. Castel, "Experimental and analytical study of corroded shear-critical reinforced concrete beams," *Materials and Structures*, vol. 47, no. 9, pp. 1467–1481, 2014.

[7] Z. Ye, W. Zhang, and X. Gu, "Deterioration of shear behavior of corroded reinforced concrete beams," *Engineering Structures*, vol. 168, pp. 708–720, 2018.

[8] Y. X. Zhao and W. L. Jin, "Analysis of the shear capacity of corroded stirrup concrete beams," *Journal of Zhejiang University*, vol. 42, no. 1, pp. 19–24, 2008, in Chinese.

[9] S. H. Xu and D. T. Liu, "The shear behavior of corroded simply supported reinforced concrete beam," *Journal of Building Structures*, vol. 25, pp. 98–104, 2004.

[10] C. Higgins and W. C. Farrow, "Tests of reinforced concrete beams with corrosion-damaged stirrups," *ACI Structural Journal*, vol. 103, pp. 133–141, 2006.

[11] Y. H. Huo, "Study on shear capacity of corroded reinforced concrete beam," *Industrial Building*, vol. 36, no. S1, pp. 910–912, 2006, in Chinese.

[12] X. H. Wang, X. H. Gao, B. Li, and B. R. Deng, "Effect of bond and corrosion within partial length on shear behaviour and load capacity of RC beam," *Construction and Building Materials*, vol. 25, no. 4, pp. 1812–1823, 2011.

[13] M. Dai, O. Yang, Y. Xiao, and F. Li, "Influence of longitudinal bar corrosion on impact behavior of RC beams," *Materials and Structures*, vol. 49, no. 9, pp. 3579–3589, 2016.

[14] X. Xue and H. Seki, "Influence of longitudinal bar corrosion on shear behavior of RC beams," *Journal of Advanced Concrete Technology*, vol. 8, no. 2, pp. 145–156, 2010.

[15] A. K. El-Sayed, "Shear capacity assessment of reinforced concrete beams with corroded stirrups," *Construction and Building Materials*, vol. 134, pp. 176–184, 2017.

[16] A. Alaskar, A. S. Alqarni, G. Alfalah, A. K. E. Sayed, H. Mohammadhosseini, and R. Alyousef, "Performance evaluation of reinforced concrete beams with corroded web reinforcement: experimental and theoretical study," *Journal of Building Engineering*, vol. 35, Article ID 102038, 2021.

[17] S. B. Li, X. Zhang, and L. D. Jia, "Analysis of the shear capacity of reinforced concrete beams with stirrup corrosion," *Journal of Engineering Mechanics*, vol. 28, no. S1, pp. 60–63, 2011, in Chinese.

[18] B. Yu and B. Chen, "A probabilistic model for calculating shear capacity of corroded reinforced concrete beams,"

Journal of Engineering Mechanics, vol. 35, no. 11, pp. 115–124, 2012, in Chinese.

[19] R. A. Hawileh, H. A. Musto, J. A. Abdalla, and M. Z. Naser, "Finite element modeling of reinforced concrete beams externally strengthened in flexure with side-bonded FRP laminates," *Composites Part B: Engineering*, vol. 173, Article ID 106952, 2019.

[20] M. Z. Naser, R. A. Hawileh, and J. Abdalla, "Modeling strategies of finite element simulation of reinforced concrete beams strengthened with frp: a review," *Journal of Composites Science*, vol. 5, no. 1, 2021.

[21] JIS-G-3112, *Japanese Industrial Standard: Steel Bars for Concrete Reinforcement*, Japanese Standard Association, Tokyo, Japan, 2004.

[22] JASS5, *Japanese Architectural Standard Specification for Reinforced Concrete Work JASS5*, Architectural Society of Japan, Tokyo, Japan, 2009.

[23] W. Zhu, R. François, D. Coronelli, and D. Cleland, "Effect of corrosion of reinforcement on the mechanical behaviour of highly corroded RC beams," *Engineering Structures*, vol. 56, pp. 544–554, 2013.

[24] B. Zhang, H. Zhu, J. Chen, and O. Yang, "Evaluation of bond performance of corroded steel bars in concrete after high temperature exposure," *Engineering Structures*, vol. 198, Article ID 109479, 2019.

[25] R. J. Zhang, A. Castel, and R. François, "Concrete cover cracking with reinforcement corrosion of RC beam during chloride-induced corrosion process," *Cement and Concrete Research*, vol. 40, no. 3, pp. 415–425, 2009.

[26] GB 50010-2010, *Code for Design of Concrete Structures*, China Building Industry Press, Beijing, China, 2010.

[27] ACI 318-08, "Building code requirements for structural concrete and commentary," *Farmington Hills: ACI Committee*, vol. 318, 2008.

[28] EN 1992-1-1, "Eurocode2: Design of Concrete Structures," *Part 1-1: General Rules and Rules for Buildings*, British Standards, Brussels, Belgium, 2004.

[29] W. W. Wei, J. X. Gong, and L. Tian, "Comparative analysis of shear bearing capacity of reinforced concrete members," *Journal of Building Science and Engineering*, vol. 27, no. 2, pp. 25–37, 2010, in Chinese.

[30] J. Xia, W. L. Jin, and L. Y. Li, "Shear performance of reinforced concrete beams with corroded stirrups in chloride environment," *Corrosion Science*, vol. 53, no. 5, pp. 1794–1805, 2011.

[31] X. M. Yang, T. Wu, and Y. Y. Wang, "Experimental study on shear behavior of reinforced concrete beams with small shear span ratio corroded," *Journal of Building Structures*, vol. 40, no. 12, pp. 147–154, 2019, in Chinese.

[32] L. Wang, X. Zhang, J. Zhang, Y. Ma, and Y. Liu, "Effects of stirrup and inclined bar corrosion on shear behavior of RC beams," *Construction and Building Materials*, vol. 98, pp. 537–546, 2015.

[33] F. J. Yu, *Experimental Study and Analysis on Performance of the Inclined Section of Corroded Reinforced concrete Beams*, Hohai University, Nanjing, China, 2005, in Chinese.

[34] Z. H. Lu, Y. B. Ou, Y. G. Zhao, and C. Q. Li, "Investigation of corrosion of steel stirrups in reinforced concrete structures," *Construction and Building Materials*, vol. 127, pp. 293–305, 2016.

[35] J. Lubliner, J. Oliver, S. Oller, and E. Oñate, "A plastic-damage model for concrete," *International Journal of Solids and Structures*, vol. 25, no. 3, pp. 299–326, 1989.

[36] B. Alfarah, F. A. López, and S. Oller, "New methodology for calculating damage variables evolution in plastic damage model for RC structures," *Engineering Structures*, vol. 132, pp. 70–86, 2017.

[37] J. Yu, W. Zhang, Z. Tang, X. Guo, and S. Pospíšil, "Seismic behavior of precast concrete beam-column joints with steel strand inserts under cyclic loading," *Engineering Structures*, vol. 216, Article ID 110766, 2020.

[38] D. Li, C. Xiong, T. Huang, R. Wei, N. Han, and F. Xing, "A simplified constitutive model for corroded steel bars," *Construction and Building Materials*, vol. 186, pp. 11–19, 2018.

[39] C. Zeng, J. H. Zhu, C. Xiong, Y. Li, D. Li, and J. Walraven, "Analytical model for the prediction of the tensile behaviour of corroded steel bars," *Construction and Building Materials*, vol. 258, Article ID 120290, 2020.

[40] L. Berto, S. Paola, and A. Saetta, "Numerical modelling of bond behavior in RC structures affected by reinforcement corrosion," *Engineering Structures*, vol. 30, no. 5, pp. 1375–1385, 2007.

[41] T. Potisuk, C. C. Higgins, T. H. Miller, and S. C. Yim, "Finite element analysis of reinforced concrete beams with corrosion subjected to shear," *Advances in Civil Engineering*, vol. 2011, Article ID 706803, 14 pages, 2011.

[42] Dassault Systèmes Simulia Corporation, *ABAQUS/Analysis User's manual*, Dassault Systèmes Simulia Corporation, Johnston, RI, USA, 2014.